Regular Article

PHYSICAL CHEMISTRY RESEARCH
Published by the
Iranian Chemical Society
www.physchemres.org
info@physchemres.org

Phys. Chem. Res., Vol. 5, No. 4, 709-725, December 2017
DOI: 10.22036/pcr.2017.82104.1368

Quantum Mechanical Approach for the Catalytic Mechanism of Dinuclear Zinc Metallo-β-lactamase by Penicillin and Cephalexin: Kinetic and Thermodynamic Points of View

M. Ghiasi[a,*] B. Noohi[a] and M. Zahedi[b]

[a]*Department of Chemistry, Faculty of Physics & Chemistry, Alzahra University, 19835-389, Vanak, Tehran, Iran*
[b]*Department of Chemistry, Faculty of Science, Shahid Beheshti University, G. C., Evin, 19839-63113, Tehran, Iran*
(Received 15 April 2017, Accepted 29 July 2017)

Metallo-β-lactamases (MβL) are catalyzing the hydrolytic cleavage of the four-membered β-lactam ring in broad spectrum of antibiotics and therefore inactivating the drug. Electronic structure and electronic energy of metallo-β-lactamase active center, two inhibitors of this enzyme including penicillin and cephalexin, and different complexes between these inhibitors and active center of metallo-β-lactamase have been investigated. For both substrates (S), the nucleophilic attack of the amide group substrate to model of active site dinuclear zinc (E) formed an ES reactive complex that by passing through the first transition state (TS1), first intermediate (INT1), the second intermediate (INT2) and second transition state (TS2) converted to the product. Also, all thermodynamic functions, ΔH^o, ΔS^o and ΔG^o, are calculated at 25 °C and 1 atm, in order to form two transition states, TS1 and TS2, and also for the total reaction of two MβL inhibitors. In all calculations, solvent effects have been considered in water using PCM method.

Keywords: Dinuclear zinc metallo-β-lactamase, Penicillin, Cephalexin, Thermodynamic functions, QM calculation

INTRODUCTION

Metallo-β-lactamases (MβLs) are bacterial enzymes that catalyze the hydrolytic cleavage of the four-membered β-lactam ring and inactivate most of the known β-lactam antibiotics [1-5]. Metallo-β-lactamase contains one or two Zn^{2+} ions in its active sites [6-10] as cofactors for the catalytic activity [11-15]. One zinc ion (Zn_1^{2+}) is coordinated to three histidine residues (His82, His84 and His145) and a bridging hydroxide ion , Water 1, [16-19], that is reminiscent of the carbonic anhydrase II active center and are arranged in a distorted tetrahedral shape [20-24]. The second zinc ion (Zn_2^{2+}) coordinates to five ligands including an aspartate (Asp86), a cystein (Cys 164), a histidin (His206), apical water (Water 2), and Water 1 [16-19] in a distorted trigonal bipyramidal geometry [21,22], Fig. 1.

Besides the extensive experimental studies [25-30], several theoretical studies on MβLs have been reported to point out the coordination structure of the active dinuclear zinc site [31,32], the catalytic mechanism and ligand binding [33,34]. However, the action mechanisms of these enzymes are still not well understood [35-38], and studies about interaction between metallo-β-lactamases and different antibiotics as a substrate of the enzymes are rare. Despite much progress in antibiotic design throughout the past 6 decades, their resistance to β-lactams is now a serious clinical problem, particularly in postsurgery, nosocomial infections and immunosupressed patients [39-42].

Four elementary reaction steps were proposed by Wang *et al.* [43-46] for kinetic mechanism of the CcrA enzyme. CcrA is a kind of MβL enzyme and this name is kind of gene coding, reaction 1,

*Corresponding author. E-mail: ghiasi@alzahra.ac.ir

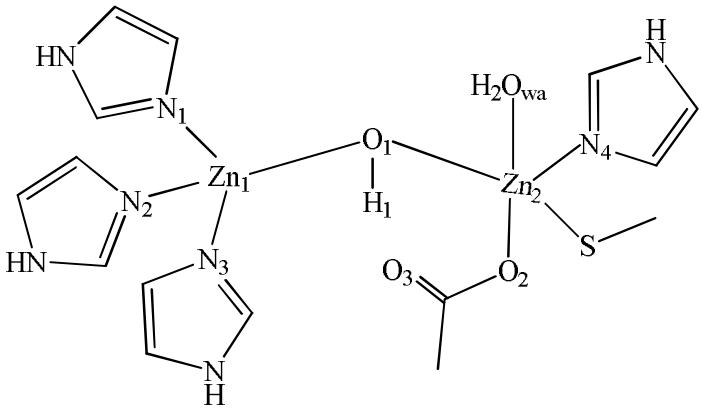

Fig. 1. Model system for the dinuclear zinc cluster of CcrA enzyme with numbering for some key atoms.

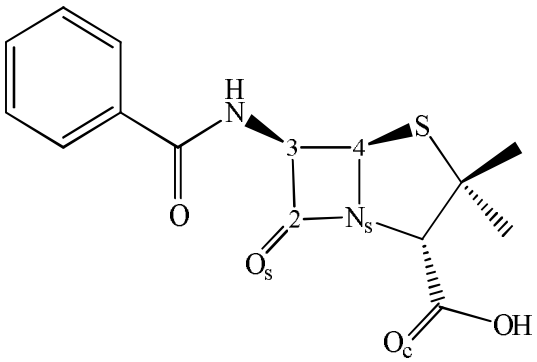

(a) Penicillin

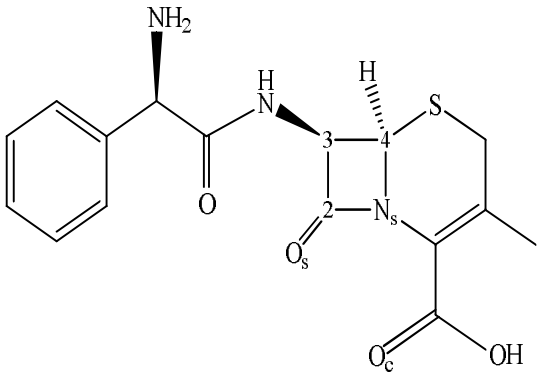

(b) Cephalexin

Fig. 2. Chemical structure of two substrates (a) penicillin and (b) cephalexin with numbering for some key atoms.

$$E + S \longleftrightarrow ES \longrightarrow EI \longrightarrow EP \longleftrightarrow E+P \quad (1)$$

which E, S and P stand for enzyme, substrate and product, respectively, and ES, EI and EP refer to complex between enzyme and substrate, intermediate and complex, and between enzyme and product, respectively. They found that the first and the fourth steps, substrate binding and product release, are rapid [31].

Taking aforementioned fact into consideration, here, we are particularly interested in studying the second and the third steps which include the nucleophilic attack of the bridging hydroxide ion on the substrate and eventual protonation of the leaving amine group [28,36]. The model system which has been employed in this study contains a hydroxide bridged dinuclear zinc cluster that is coordinated to imidazole molecule, acetate and thiolate ions, Fig. 1. Subsequently, the inhibition mechanism, potential energy profile, the stationary state, intermediate and transition structures according to reaction model 1 for the CcrA enzyme by two antibiotics containing penicillin and cephalexin have been investigated, Fig. 2.

COMPUTATIONAL METHODS

All calculations were performed using the Gaussian 98 [47] software. The optimization of dinuclear zinc metallo-β-lactamase (MβL) model and inhibitors, the complex between inhibitors and MβL, including intermediate and transition state geometries were done at the B3LYP-D3 level [48,49] employing the standard 6-31G basis set. Full optimizations were performed without any symmetry constrains. We use the STABLE keyword to confirm the most stable conformer of all compounds. The harmonic vibrational frequencies were computed to confirm that the optimized geometry correctly corresponds to a local minimum that has only real frequencies. The SCAN and QST3 procedure was used to search for transition states. All TS geometries were double checked using IRC and FREQ calculations. In addition, the thermodynamic properties of all compounds were obtained from frequency calculations at 298.15 K and 1.0 atmosphere pressure. All reported enthalpies were zero-point (ZPE) corrected with unscaled frequencies.

The solvent effects on the conformational equilibrium and contribution to the total enthalpies were investigated with PCM method [50]. Solvation calculations were carried out for water with the geometry optimization for this solvent.

RESULTS AND DISCUSSION

Geometry Optimization

Geometry optimization of active site dinuclear zinc cluster of the CcrA enzyme (DZCC). The model system for the active site dinuclear zinc cluster of the CcrA enzyme was optimized at B3LYP-D3/6-31G level, with no initial symmetry restrictions and assuming C_1 point group. Calculation of vibrational frequencies has confirmed stationary point with no negative eigenvalue in the force constant matrix. The optimized geometry of DZCC active center in the gas phase was reoptimized by considering the solvent effect ($\epsilon = 78.9$) using PCM method [50] at the same level of calculation. The calculated results indicate that DZCC active center is stabilized by about 56.47 kcal mol^{-1} in the water solvent.

Figure 3 shows the optimized geometry of active site dinuclear zinc cluster of the CcrA enzyme at the B3LYP-D3/6-31G level while some structural details of DZCC active site are presented in Table 1 for the gas and solvent phases.

Geometry optimization of penicillin and cephalexin. Two inhibitors, penicillin and cephalexin, Fig. 2, have been fully optimized in the gas phase, and then in the water solvent at the same level of calculation for DZCC active center. The calculated results indicate that the two substrates are stabilized by 12.55 and 18.82 kcal mol^{-1}, respectively, in the water solvent.

Figure 4 shows the optimized geometry of the two inhibitors in the water solvent. The results of frequency calculations confirm the stationary points of two inhibitors. Some structural details of the inhibitors are presented in Table 2.

Nucleophilic Attack of the Substrate Amide Group to Active Site Dinuclear Zinc Cluster of the CcrA:

According to Fig. 5, the substrate amide group attacks to zinc ion (Zn1) by the bridging hydroxide ion, and then the reaction intermediate is hydrolyzed by an external water

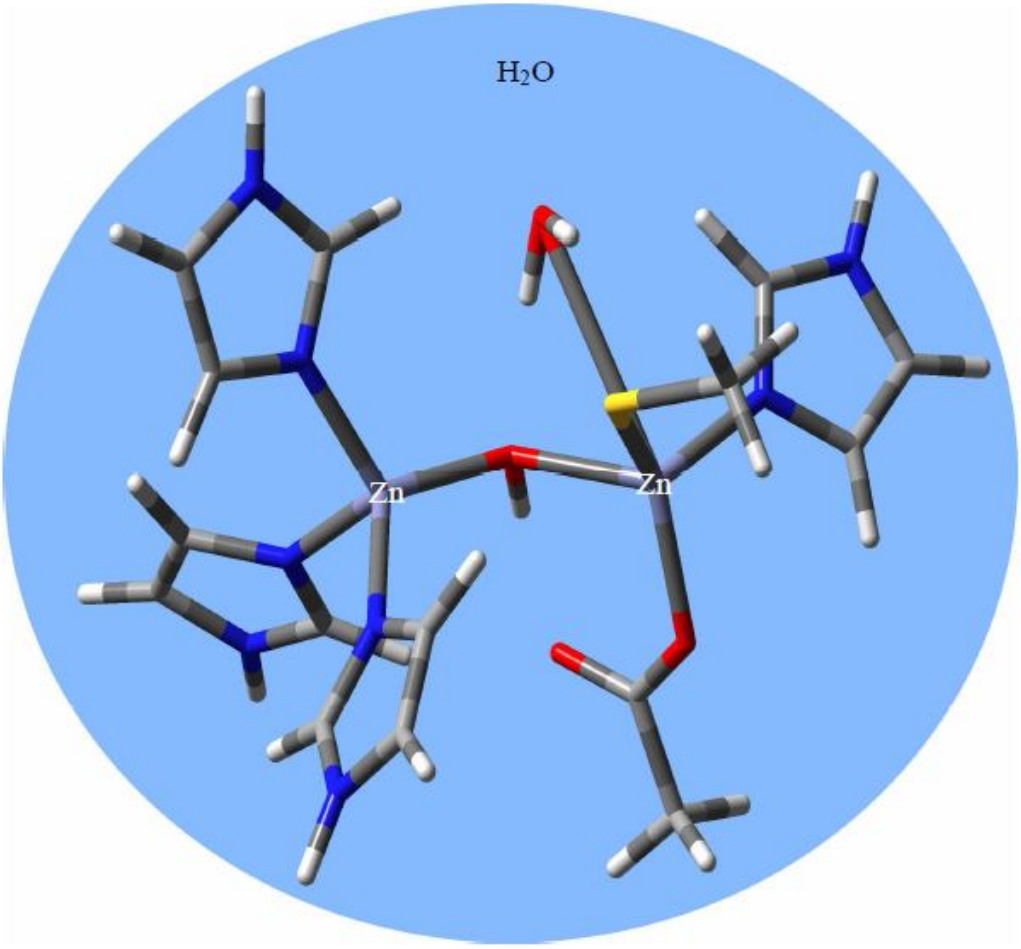

Fig. 3. Optimized structure for active site of dinuclear zinc cluster of CcrA enzyme' model in water solvent.

molecule to produce the product. The ES complexes were constructed from the optimized geometry of DZCC, penicillin and cephalexin and optimized in the gas and water phases. The result of calculations indicates that penicillin and cephalexin are bound to the active center through direct coordination of the amino carbonyl oxygen (Os in Fig. 2) substrates to Zn1. Also, calculated results show that the optimum distances of Os-Zn1 in the reactive (DZCC/ Penicillin) and (DZCC/Cephalexin) complexes are 2.68 Å and 2.70 Å, respectively. The Os...Zn1 interaction, similar to the role of a Lewis acid catalyst in the amid hydrolysis reaction, polarizes the carbonyl bond [51,52]. Therefore, the susceptibility of the amino carbonyl carbon substrate is increased towards nucleophilic attack. After optimization of these two reactive complexes, the apical water ligand (Water 2) was replaced by the penicillin and cephalexin carboxylate groups, and then the bridging hydroxide ion was migrated from Zn2, and was stabilized at a distance of about 5 Å for penicillin and cephalexin, respectively, to assume a suitable orientation for the nucleophilic attack on the amino carbonyl carbon. The stabilization energy to form the reactive complex (ES) is about 10.0 kcal mol^{-1} for both inhibitors.

From the optimized reactive complexes, (DZCC/ Penicillin) and (DZCC/Cephalexin), as a starting point the C2-Ns bond in β-lactam in penicillin and cephalexin is increased from 1.2 Å and 1.3 Å in step of 0.1 Å and simultaneously the O1 (Water 1)....C2 distance is reduced

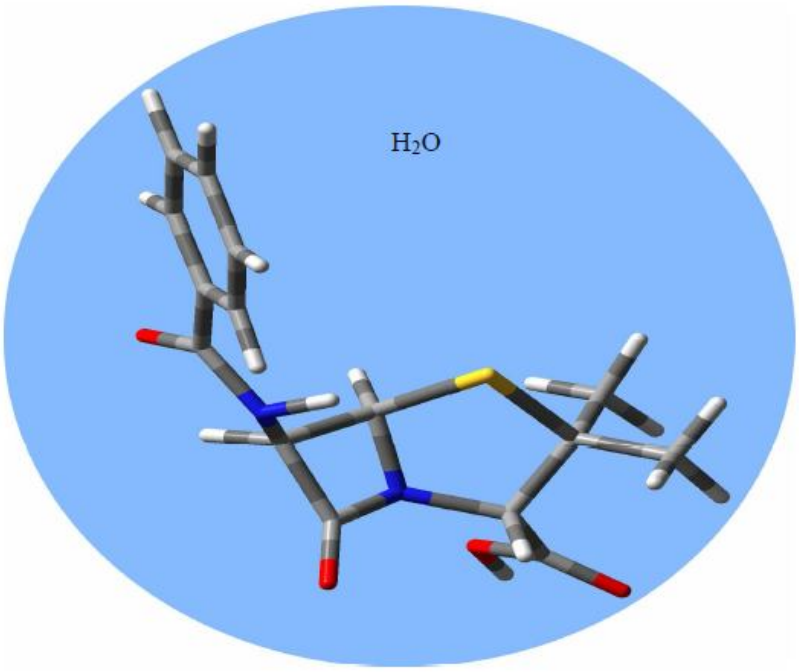

(a) Penicillin

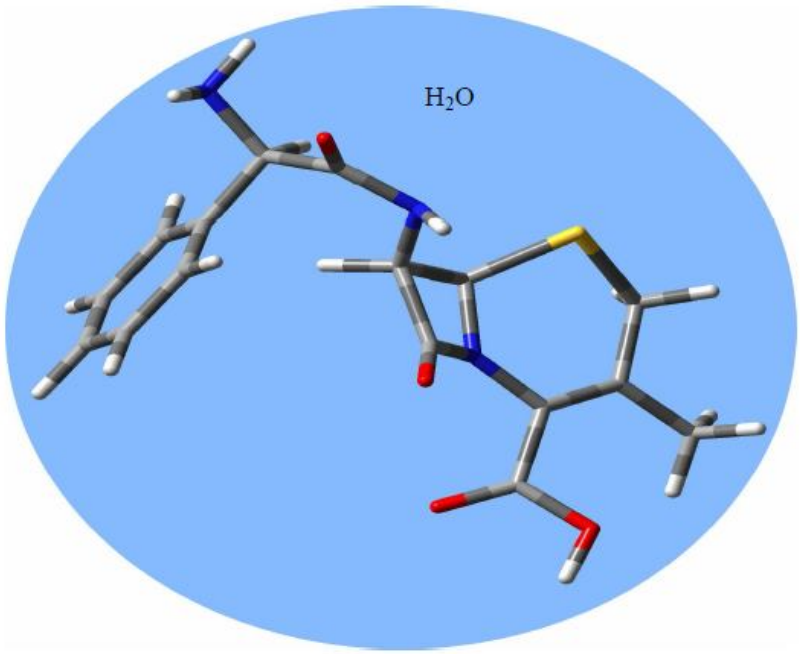

(b) Cephalexin

Fig. 4. Optimized structure of (a) penicillin and (b) cephalexin in water solvent.

Table 1. Some Structural Details for Active Site of Dinuclear Zinc Cluster of CcrA Enzyme' Model in Solution and Gas Phase (in the Parenthesis) at B3LYP-D3/6-31G Level

Connected atoms		
Bond distance (Å)		Exp.
Zn1-O1	1.94(1.94)	1.90
Zn1-N1	2.01(2.01)	2.00
Zn1-N2	2.04(2.03)	2.10
Zn1-N3	2.02(2.02)	2.00
Zn2-O1	2.03(2.03)	2.10
Zn2-O2	1.98(1.98)	2.10
Zn2-Owa	3.23(3.22)	2.30
Zn2-S	2.34(2.34)	2.30
Zn2-N4	2.02(2.01)	2.10
Standard deviation	0.99(0.99)	
Bond angle (°)		
Zn1-O1-Zn2	127.22(126.98)	125.10
O1-Zn2-O2	99.92(100.00)	100.20
O1-Zn2-Owa	56.45(56.46)	57.00
Standard deviation	2.21	
Dihedral angle (°)		
Zn1-O1-Zn2-O2	88.52(88.52)	88.90
Zn1-O1-Zn2-Owa	-107.50(-107.51)	-107.5
Zn1-O1-Zn2-S	-46.61(-46.58)	-47.3
Zn1-O1-Zn2-N4	-167.82(-167.82)	-167.20
Standard deviation	1.00(1.00)	

Table 2. Some Structural Details of Penicillin and Cephalexin in Solution and Gas Phase (in the Parenthesis)

Compound	Connected atoms	
	Bond distance(Å)	
	Os-C2	1.23(1.22)
	C2-C3	1.56(1.57)
	C3-C4	1.57(1.56)
	C4-N5	1.47(1.48)
	Ns-C2	1.41(1.41)
Penicillin	Bond angle (°)	
	Os-C2-C3	137.22(137.20)
	C2-C3-C4	84.72(83.12)
	C3-C4-Ns	88.36(87.49)
	Ns-C2-Os	131.35(130.46)
	Dihedral angle (°)	
	Os-C2-Ns-C4	-165.12(-163.67)
	Os-C2-C3-C4	165.22(163.87)
	C2-C3-C4-Ns	9.06(6.78)
	Bond distance (Å)	
	Os-C2	1.22(1.23)
	C2-C3	1.56(1.57)
	C3-C4	1.58(1.58)
	C4-Ns	1.46(1.46)
	Ns-C2	1.41(1.40)
Cephalexin	Bond angle (°)	
	Os-C2-C3	135.97(136.11)
	C2-C3-C4	84.94(85.10)
	C3-C4-Ns	88.08(88.67)
	Ns-C2-Os	133.13(134.00)
	Dihedral angle (°)	
	Os-C2-Ns-C4	-167.59(-167.11)
	Os-C2-C3-C4	167.98(168.00)
	C2-C3-C4-Ns	7.30(7.65)

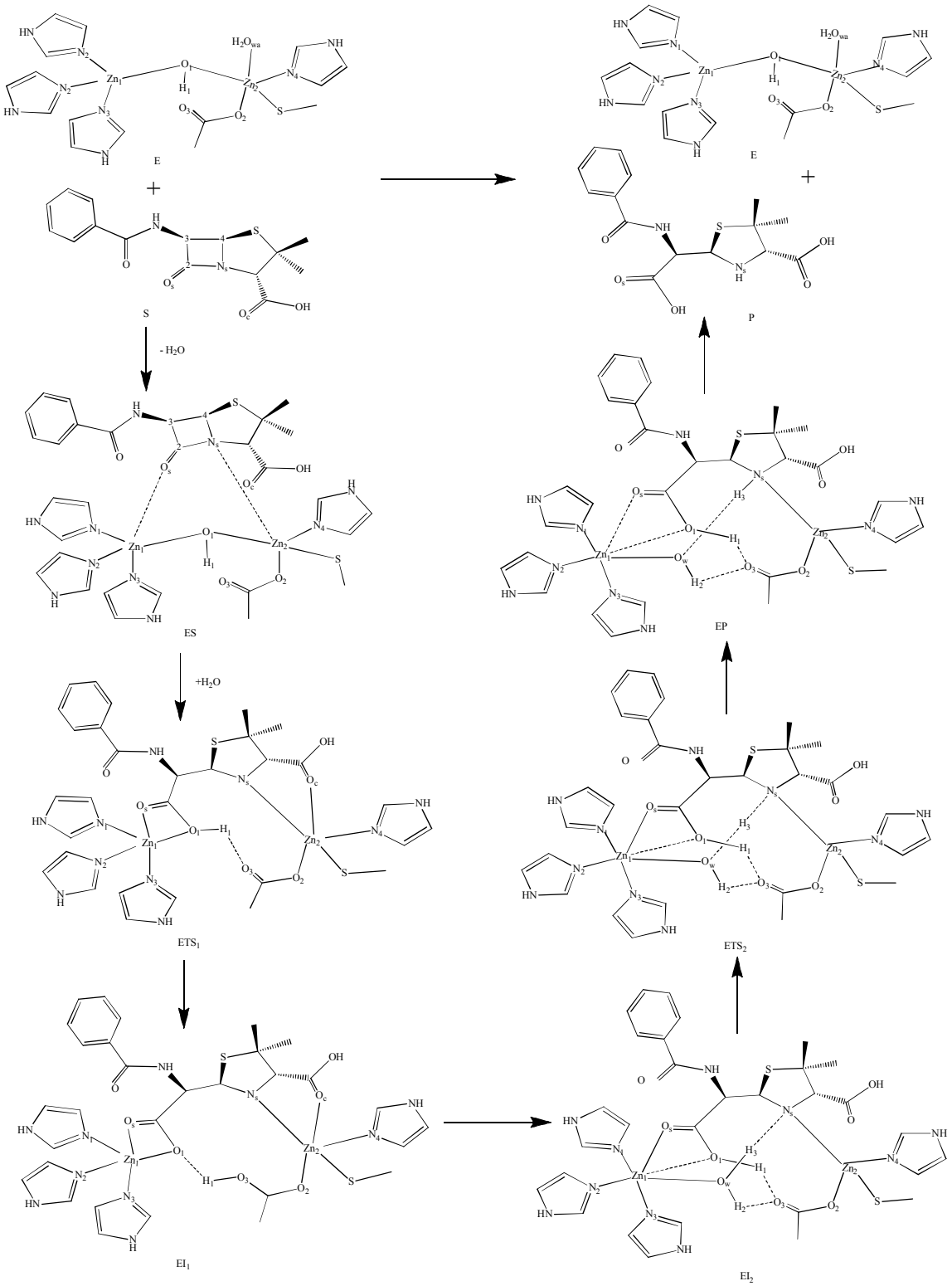

Fig. 5. Reaction model for nucleophilic attack of the substrate amide group to the dinuclear zinc cluster of CcrA enzyme' model.

from 4 Å and 4.2 Å in step of 0.3 Å. The system passes through the first transition state when the C2-Ns bond in penicillin and cephalexin has been broken and the C2….O1 bond is formed (1.66 Å and 1.71 Å in penicillin and cephalexin respectively). This geometry has been optimized in the water as a first transition state (TS1) for both substrates. One imaginary frequency (-23.45 cm^{-1} and -26.78 cm^{-1} for penicillin and cephalexin antibiotic, respectively) in frequency calculation confirms the transition state. The barrier energy from ES complex to TS1 is 6.50 kcal mol^{-1} and 8.60 kcal mol^{-1} for penicillin and cephalexin, respectively, Figs. 6 and 7. When the O1-C2 bond is completely formed and the C2-Ns bond is fully broken, the system arrives at the intermediate (INT1). In this geometry, deprotonated nitrogen atom (Ns) interacts with Zn2, while the Ns…Zn2 distance is 2.0 Å for both penicillin and cephalexin, respectively. Our results are confirmed by the experimental observation for the anionic intermediate bound to a zinc ion in the catalytic reaction of B.fragilis enzyme and its functional mimics [43,53]. The geometry of the first transition state, TS1 has been confirmed using QST3 procedure between the reactive complex and the first intermediate. Some electronic structural details of the reactive complex, the first transition state and the first intermediate are presented in Table 3.

According to the previous studies [43,54], the second catalytic reaction step contains proton transfer from the bulk solvent. Therefore, in the next step to form the second intermediate (INT2), the water molecule was added to the first intermediate, while the distances between water molecule and Zn1 and Zn2 were equal, and then the structure was optimized at the same level of calculation. Our results suggest that Zn1 prefers to be hydrated rather than Zn2 in both (DZCC/Penicillin) and the (DZCC/Cephalexin) intermediate complexes. According to Fig. 5, the EP complexes for both of the antibiotics were constructed and optimized in the water solvent. The second transition state between the second intermediate and the EP complex has been found by using QST3 producer for both antibiotics. The results of frequency calculation with one imaginary frequency (-30.78 cm^{-1} and -32.56 cm^{-1} for penicillin and cephalexin, respectively) confirm the transition state geometry for both antibiotics. The imaginary frequency corresponds to the curvature in the transition state region along the reaction coordinate. The low barrier corresponds to a small curvature along the reaction coordinate in the region of TS, and so the imaginary frequency will be likely to be small. Conversely, the big barrier corresponds to a large reaction coordinate near the TS, and to a large imaginary frequency.

Considering the solvent effect, variation of the potential energy for this reaction path for both antibiotics is presented in Figs. 6 and 7. The energy barrier between INT2 and TS2 is about 4.90 kcal mol^{-1} and 5.70 kcal mol^{-1} for penicillin and cephalexin, respectively, in solution phase. Some selected geometrical parameters for INT2, TS2 and EP for both antibiotics are complied in Table 3. The stabilization energy between EP complex and optimized reaction products for penicillin and cephalexin in the water solvent is about 10.36 and 9.23 kcal mol^{-1}, respectively. Also, IRC potential energy curves have been reported in Figures S1 to S4 in supplementary information.

Calculation of the Thermodynamic Functions

For both inhibitors, no experimental data are available for the thermodynamic functions, such as standard enthalpies of reaction (ΔH^{o}_{rxn}) and the standard Gibbs free energies of reaction (ΔG^{o}_{rxn}) . So ΔU^{o}_{rxn}, ΔH^{o}_{rxn}, ΔS^{o}_{rxn} and ΔG^{o}_{rxn} were calculated for both antibiotics according to the total reaction in Fig. 5.

Total enthalpies of the studied species X, H(X), at the temperature T are usually estimated from the Eq. (2) [55-57],

$$H(X) = E_0 + ZPE + E_{trans} + E_{rot} + E_{vib} + RT \quad (2)$$

where E_0 is the calculated total electronic energy, ZEP stands for zero-point energy, E_{trans}, E_{rot}, E_{vib} are the translational, rotational, and vibrational contributions to the enthalpy, respectively. Finally, RT represents PV-work term and is added to convert the energy to enthalpy.

The standard enthalpy change of the reaction (ΔH^{o}_{rxn}) is given as:

$$\Delta H^{o}_{rxn} = (H^{\circ}_{product}) - (H^{\circ}_{reactant}) \quad (3)$$

which total standard enthalpies of the studied species, at the temperature T were estimated from the expression (2).

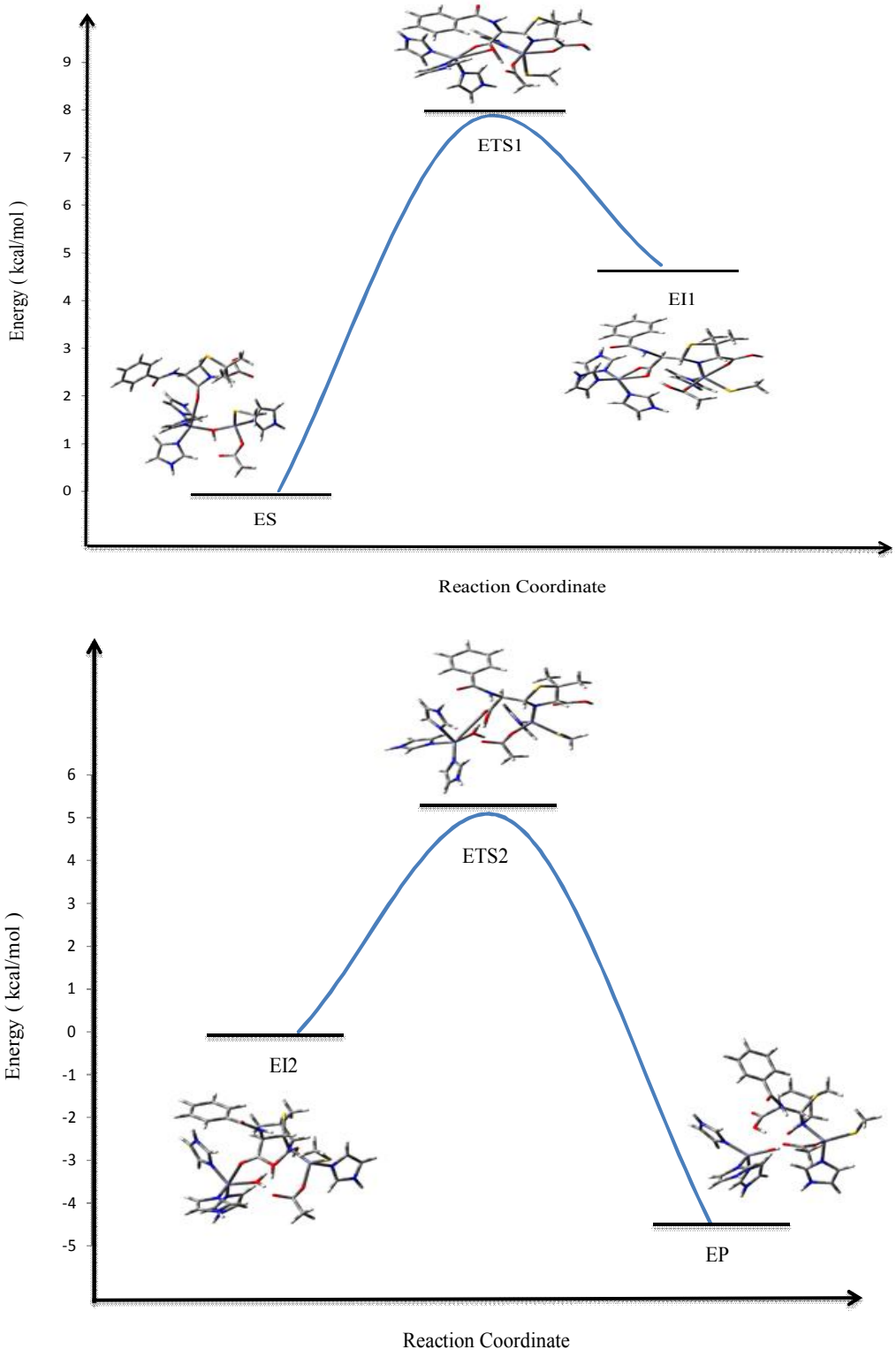

Fig. 6. Presentation of potential energy profiles for the nucleophilic substitution reaction step (left) and for the proton transfer reaction step (right) of the enzymatic reaction model for penicillin.

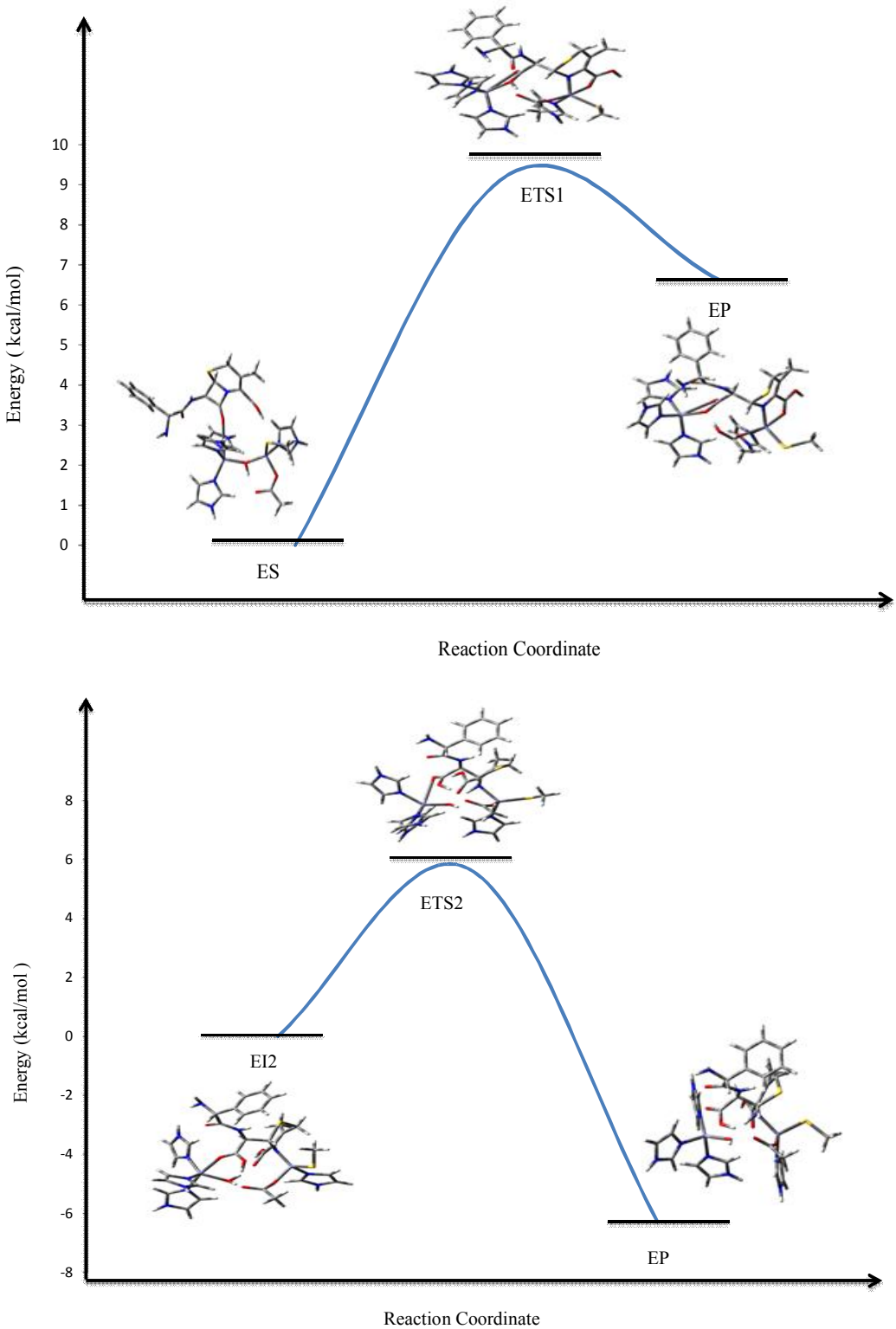

Fig. 7. Presentation of potential energy profiles for the nucleophilic substitution reaction step (left) and for the proton transfer reaction step (right) of the enzymatic reaction model for cefalexin.

Table 3. Some Structural Details of Different Complexes Through the Reaction Path for Penicillin and Cephalexin in Solution Phase

Compound	Bond distance (Å)	ES	ETS1	EI1	EI2	ETS2	EP
Penicillin	Zn1-O1	1.95	2.15	2.62	2.95	2.31	3.20
	Zn2-O1	2.00	3.10	4.0	-	-	-
	Os-Zn1	2.68	2.23	2.12	2.63	2.47	2.78
	Ns-Zn2	4.91	2.56	2.00	2.01	2.20	2.31
	H1-O3	1.75	1.62	1.00	1.67	1.82	1.73
	H1-O1	-	-	1.60	-	-	-
	Oc-Zn2	-	-	2.40	-	-	-
	Zn1-Ow	-	-	-	2.00	1.95	1.91
	H2-O3	-	-	-	1.60	1.67	2.01
	H3-Ns	-	-	-	2.62	1.97	-
	H3-Ow	-	-	-	1.12	1.67	2.00
Cephalexin	Zn1-O1	1.94	2.24	2.22	3.21	2.41	3.54
	Zn2-O1	1.96	3.23	4.43	-	-	-
	Os-Zn1	2.70	2.34	2.57	2.30	2.52	2.98
	Ns-Zn2	5.20	2.61	2.00	2.10	2.32	2.24
	H1-O3	1.71	1.65	1.10	1.65	1.73	1.22
	H1-O1	-	-	1.63	-	-	-
	Oc-Zn2	-	-	2.32	-	-	-
	Zn1-Ow	-	-	-	2.00	1.87	1.95
	H2-O3	-	-	-	1.62	1.67	3.39
	H3-Ns	-	-	-	2.92	2.00	-
	H3-Ow	-	-	-	1.22	1.65	1.72

Table 4. Calculated Thermodynamic Functions (kcal mol^{-1}) of the Total Reaction in the Solution and in the Gas Phase (in the Parenthesis)

Thermodynamic functions	Compound	
	Penicillin	Cephalexin
$\Delta U^{\#}_1$	6.50(8.25)	8.60(11.23)
$\Delta H^{\#}_1$	6.50(8.25)	8.60(11.23)
$\Delta S^{\#}_1$	-0.02(-0.02)	-0.02(-0.02)
$\Delta G^{\#}_1$	12.46(14.21)	14.56(17.19)
$\Delta U^{\#}_2$	4.90(7.34)	5.70(8.45)
$\Delta H^{\#}_2$	4.90(7.34)	5.70(8.45)
$\Delta S^{\#}_2$	-0.01(-0.01)	-0.01(-0.01)
$\Delta G^{\#}_2$	7.88(10.32)	8.68(11.43)

Table 5. Calculated Thermodynamic Functions (kcal mol^{-1}) of the Different Complexes through the Reaction Path in the Solution and in the Gas Phase (in the Parenthesis)

Thermodynamic functions	Compound	
	Penicillin	Cephalexin
$\Delta U^{\#}_1$	6.50(8.25)	8.60(11.23)
$\Delta H^{\#}_1$	6.50(8.25)	8.60(11.23)
$\Delta S^{\#}_1$	-0.02(-0.02)	-0.02(-0.02)
$\Delta G^{\#}_1$	12.46(14.21)	14.56(17.19)
$\Delta U^{\#}_2$	4.90(7.34)	5.70(8.45)
$\Delta H^{\#}_2$	4.90(7.34)	5.70(8.45)
$\Delta S^{\#}_2$	-0.01(-0.01)	-0.01(-0.01)
$\Delta G^{\#}_2$	7.88(10.32)	8.68(11.43)

Similarity, ΔS°_{rxn} could be obtained by

$$\Delta S^{\circ}_{rxn} = (S^{\circ}_{product}) - (S^{\circ}_{reactant}) \quad (4)$$

According to the thermodynamic equation, $\Delta G = \Delta H - T\Delta S$, the ΔG°_{rxn} was calculated.

The calculated thermodynamic properties of the total reaction for both antibiotics in gas and solution phase are reported in Table 4.

The negative values of ΔH°_{rxn} and ΔG°_{rxn} for both substrates in both gas and solution phases indicate the exothermicity and spontaneity of the desired reaction for both penicillin and cephalexin molecules. Moreover, the most apparent effect of the solvent with more negative value of reaction enthalpy is that reactants and products are stabilized, however, the products are more stabilized due to the stronger solute-solvent interaction than the reactants.

According to the results presented in Table 5, the calculated activation free energies, $\Delta G^{\neq}$, for TS1 and TS2 are 12.46 (14.21) and 7.88 (10.32) kcal mol^{-1} for penicillin and 14.65 (17.19) and 8.68 (11.43) kcal mol^{-1} for cephalexin, respectively, The values in the parentheses refer to the gas phase calculation. Also, activation enthalpy same as the activation free energy of the first and second transition states in the reaction path in solution phase is lower in energy then the gas phase values which is due to the more stabilization of the transition states rather than intermediates in the water solvent. On the basis of these results, it is suggested that the C-N bond cleavage for both antibiotics could be the rate-limiting step of the reaction.

CONCLUSIONS

Metallo-β-lactamases cause bacterial resistance toward a different kind of β-lactam antibiotics by catalyzing the hydrolytic cleavage of the four-membered ring of β-lactame and inactivating the drug. In the present study, the quantum mechanical calculations have been applied to study the reaction mechanism used by metallo-β-lactamases CcrA from B.fragilis in complex with penicillin and cephalexin antibiotics. The studied energy profile for two antibiotics indicates a two-stepwise mechanism. The details of electronic structures and energetic profile of the active site model indicate that the two zinc ions, Zn1 and Zn2, have an important role in catalysis. The active site zinc ion (Zn1) provides a suitable site to bind the antibiotics amino carbonyl oxygen to form the reactive complex. According to the calculated potential energy surface, two transition states and two intermediates have been found in the catalyzed pathway. Overall, passing through the second transition state, the reacting system falls into the energy minimum EP and the final energy minimum products. In addition, our theoretical study is valuable not only to get an insight into the reaction, but also to provide the details of molecular mechanism, electronic, structural and thermodynamic information of the species appearing along the enzymatic reaction through synthesis of the new antibiotics.

ACKNOWLEDGMENTS

The authors gratefully acknowledge financial support from the research council of Alzahra University. Technical support of the Chemistry Computation Center at Shahid Beheshti University is greatly acknowledged.

REFERENCES

[1] Brown, N. G.; Horton, L. B.; Huang, W.; Vongpunsawad, S.; Palzkill1, T., Analysis of the functional contributions of Asn233 in Metallo-β-Lactamase IMP-1, *Antimicrob. Agents Chemother* **2011**, *55*, 5696-5702, DOI: 10.1128/AAC.00340-11.

[2] Ackerman, S. H.; Gatti, D. L., Biapenem inactivation by B2 metallo β-lactamases: Energy landscape of the hydrolysis reaction, *PLOS ONE* **2013**, *8*, 1-14, DOI: 10.1371/journal.pone.0055136.

[3] Leiros, H. K. S.; Borra, P. S.; Brandsdal, B. O.; Edvardsen, K. S. W.; Spencer, J.; Walsh, T. R.; Samuelsen, O., Crystal structure of the mobile metallo-β-lactamase AIM-1 from Pseudomonas aeruginosa: insights into antibiotic binding and the role of Gln157, *Antimicrob. Agents Chemother* **2012**, *56*, 4341-4353, DOI: 10.1128/AAC.00448-12.

[4] Kim, Y.; Tesar, C.; Mire, J.; Jedrzejczak, R.; Binkowski, A.; Babnigg, G.; Sacchettini, J.; Joachimiak, A., Structure of apo- and monometalated forms of NDM-1-A highly potent carbapenem-hydrolyzing metallo-β-lactamase, *PLOS ONE 2011, 6*,

1-12, DOI: 10.1371/journal.pone.0024621.

[5] Bush K.; Jacoby, G. A., Updated functional classification of β-lactamases, *Antimicrob. Agents Chemother* **2010**, *54*, 969-976, DOI: 10.1128/AAC.01009-09.

[6] Thomson J. M.; Bonomo, R. A., The threat of antibiotic resistance in Gram-negative pathogenic bacteria: β-lactams in peril!, *Curr. Opin. Microbiol.* **2005**, *8*, 518-524, DOI: 10.1016/j.mib.2005.08.014.

[7] Wilke, M. S.; Lovering, A. L.; N. C. Strynadka, β-lactam antibiotic resistance: a current structural perspective, *Curr. Opin. Microbiol.* **2005**, *8*, 525-533, DOI: 10.1016/j.mib.2005.08.016.

[8] Hu, Z.; Periyannan, G. R.; Crowder, M. W., Folding strategy to prepare Co-substituted metallo-β-lactamas L1, *Anal. Biochem.* **2008**, *378*, 177-183, DOI: 10.1016/j.ab.2008.04.007.

[9] Bush, K.; Jacoby, G. A., Updated functional classification of β-lactamases, *Antimicrob. Agents Chemother.* **2010**, *54*, 969-976, DOI: 10.1128/AAC.01009-09.

[10] Leiros, S.; Borra, P. S.; Brandsdal, B. O.; Edvardsen, K. S. W.; Spencer, J.; Walsh, T. R.; Samuelsen, Ø., Crystal structure of the mobile metallo-β-lactamase AIM-1 from Pseudomonas aeruginosa: Insights into antibiotic binding and the role of Gln157, *Antimicrob. Agents Chemother* **2012**, *56*, 4341-4353, DOI:

[11] Wang, J. F.; Chou, K. C., Insights from modeling the 3D structure of new delhi metallo-β-lactamse and its binding interactions with antibiotic drugs, *PLOS ONE* **2011**, *6*, 1-6, DOI: 10.1371/journal.pone.0018414.

[12] Barrio, J. M.; Lisa, M. N.; Vila, A. J., *In vivo* impact of Met221 substitution in GOB metallo-β-lactamase, *Antimicrob. Agents Chemother* **2012**, *56*, 1769-1773, DOI: 10.1128/AAC.05418-11.

[13] Oelschlaeger, P.; Mayo, S. L., Hydroxyl groups in the ββ sandwich of metallo-β-lactamase favor enzyme activity: A computational protein design study, *J. Mol. Biol.* **2005**, *350*, 395-401, DOI: 10.1016/j.jmb.2005.04.044.

[14] Hu, Z.; Periyannan, G.; Bennett, B.; Crowder, M. W., Role of the Zn1 and Zn2 sites in metallo-β-lactamase L1, *J. Am. Chem. Soc.* **2008**, *130*, 14207-14216, DOI: 10.1021/ja8035916.

[15] Hall, B. G.; Salipante, S. J.; Barlow, M., Independent origins of subgroup Bl+B2 and subgroup B3 metallo-β-lactamases, *J. Mol. Evol.* **2004**, *59*, 133-141, DOI: 10.1007/s00239-003-2572-9.

[16] Li, Z.; Rasmussen, B. A.; Herzberg, O.; Structural consequences of the active site substitution Cys181 Ser in metallo-β-Lactamase from Bacteroides fragilis, *Protein Sci.* **1999**, *8*, 249-252.

[17] Laraki, N.; Franceschini, N.; Rossolini, G. M.; Santucci, P.; Meunier, C.; Pauw, E.; Amicosante, G.; Frere, J. M. Galleni, M., Biochemical characterization of the Pseudomonas aeruginosa 101/1477 metallo-beta-lactamase IMP-1 produced by Escherichia coli, *Antimicrob. Agents Chemother.* **1999**, *43*, 902-906.

[18] Chantalat, L.; Duee, E.; Galleni, M.; Frere, J. M.; Dideberg, O.; Structural effects of the active site mutation cysteine to serine in Bacillus cereus zinc-beta-lactamase, *Protein Sci.* **2000**, *9*, 1402-1406.

[19] Page, M.L.; Badarau, A.; The mechanisms of catalysis by metallo-β-lactamases, *Bioinorg. Chem. Appl.* **2008**, *38*, 71-78, DOI: 10.1155/2008/576297.

[20] Carfi, A.; Pares, S.; Duee, E.; Galleni, M.; Duez, C.; Frere, J. M.; Dideberg, O., The 3-D structure of a zinc metallo-β-lactamase from bacillus cereus reveals a new type of protein fold, *The EMBO J.* **1995**, *14*, 4914-4921.

[21] Concha, N. O.; Rasmussen, B. A.; Bush, K.; Herzberg, O., Crystal structure of the wide-spectrum binuclear zinc β-lactamase from Bacteroides fragilis, *Structure.* **1996**, *4*, 823-836, DOI: 10.1016/S0969-2126(96)00089-5.

[22] Simona, F.; Magistrato, A.; Peraro, M. D.; Cavalli, A.; Vila, A. J.; Carloni, P.; Common mechanistic features among metallo-β-Lactamases: a computational study of Aeromonas hydrophila CphA enzyme, *J. Biol. Chem.* **2009**, *284*, 28164-28171, DOI: 10.1074/jbc.M109.049502.

[23] Barrio, J. M.; Gonzalez, J. M.; Lisa, M. N.; Costello, A. L.; Peraro, M. D.; Carloni, P.; Bennett, B.; Tierney, D. L.; Limansky, A. S.; Viale, A. M.; Vila, A., The Metallo-β-Lactamase GOB is a mono-Zn enzyme with a novel active site, *J. Biol. Chem.* **2007**, *282*, 18286-18293, DOI: 10.1074/jbc.M700467200.

[24] Breece, R. M.; Hu, Z.; Bennett, B.; Crowder, M. W.;

Tierney, D. L.; Motion of the zinc ions in catalysis by a di-Zinc metallo-β-lactamase, *J. Am. Chem. Soc.* **2009**, *131*, 11642-11643, DOI: 10.1021/ja902534b.

[25] Materon, I. C.; Palzkill, T., Identification of residues critical for metallo-β-lactamase function by codon randomization and selection, *Protein Sci.* **2001**, *10*, 2556-2565, DOI: 10.1110/ps.40884.

[26] Sharma, N.; Toney, J. H.; Fitzgerald, P. M. D., Expression, purification, crystallization and preliminary X-ray analysis of Aeromonas hydrophilia metallo-β-lactamase, *Acta Cryst.* **2005**, *61*, 180-182, DOI: 10.1107/S1744309104033512.

[27] Badarau, A.; Llinas, A.; laws, A. P.; Damblon, C.; Page, M. I., Inhibitors of metallo-β-lactamase generated from β-lactam antibiotics, *Biochemistry.* **2005**, *44*, 8578-8589, DOI: 10.1021/bi050302j.

[28] Oelschlaeger, P.; Mayo, S. L.; Pleiss, J.; Impact of remote mutations on metallo-β-lactamase substrate specificity: implications for the evolution of antibiotic resistance, *Protein Sci.* **2005**, *14*, 765-774, DOI: 10.1110/ps.041093405.

[29] Sharma, N. P.; Hajdin, C.; Chandrasekar, S.; Bennett, B.; Yang, K. W.; Crowder, M. W., Mechanistic studies on the mononuclear Zn[II]-containing metallo-β-lactamase lmis from Aeromonas sobria, *Biochemistry.* **2006**, *45*, 10729-10738, DOI: 10.1021/bi060893t.

[30] Spencer, J.; Read, J.; Sessions, R. B.; Howell, S.; Blackburn, G. M.; Gamblin, S. J., Antibiotic recognition by binuclear metallo-β-lactamases revealed by X-ray crystallography, *J. Am. Chem. Soc.* **2005**, *127*, 14439-14444, DOI: 10.1021/ja0536062.

[31] Park, H.; Brothers, E. N.; Merz, K. M.; Hybrid QM/MM and DFT Investigations of the Catalytic Mechanism and Inhibition of the Dinuclear Zinc Metallo-β-Lactamase CcrA from Bacteroides fragilis, *J. Am. Chem. Soc.* **2005**, *127*, 4232-4241, DOI: 10.1021/ja042607b.

[32] Gherma, B. F.; Goldberg, S. D.; Cornish, V. W.; Friesner, R. A., Mixed Quantum mechanical/molecular mechanical [QM/MM] study of the deacylation reaction in penicillin binding protein [PBP] versus in a class C β-Lactamase, *J. AM. Chem. Soc.* **2004**, *126*, 7652-7664, DOI: 10.1021/ja036879a.

[33] Lisa, M. N.; Hemmingsen, L.; Vila, A., Catalytic role of the metal ion in the Metallo-β-Lactamase GOB, *J. Biol. Chem.* **2010**, *285*, 4570-4577, DOI: 10.1074/jbc.M109.063743.

[34] Griffin, D. H.; Richmond, T. K.; Sanchez, C.; Moller, A. J.; Breece, R. M.; Tierney, D. L.; Bennett, B.; Crowder, M. W., Structural and kinetic studies on metallo-β-lactamase IMP-1, *Biochemistry.* **2011**, *50*, 9125-9134, DOI: 10.1021/bi200839h.

[35] Costello, A.; Periyannan, G.; Yang, K. W.; Crowder, M. W.; Tierney, D. L., Site-selective binding of Zn(II) to metallo-β-lactamase L1 from Stenotrophomonas maltophilia, *Bio1 Inorg Chem.* **2006**, *11*, 351-358, DOI: 10.1007/s00775-006-0083-z.

[36] Peraro, M. D.; Vila, A. J.; Carloni, P.; Klein, M. L., Role of zinc content on the catalytic efficiency of B1 metallo-β-lactamases, *J. Am. Chem. Soc.* **2007**, *129*, 2808-2816, DOI: 10.1021/ja0657556.

[37] Xu, D.; Guo, H.; Cui, Q., Antibiotic deactivation by a dizinc β-lactamase: Mechanistic insights from QM/MM and DFT studies, *J. AM. Chem. Soc.* **2007**, *129*, 10814-10822, DOI: 10.1021/ja072532m.

[38] Crowder, M. W.; Spencer, J.; Vila, A. J.; Metallo-β-lactamases: Novel weaponry for antibiotic resistance in becteria, *Acc. Chem. Res.* **2006**, *39*, 721-728, DOI: 10.1021/ar0400241.

[39] Levy, S. B., Factors impacting on the problem of antibiotic resistance, *J. Antimicrob. Chemother.* **2002**, *49*, 25-30, DOI: 10.1093/jac/49.1.25.

[40] Al-Jasser, A. M.; Extended-spectrum beta-lactamases [ESBLs]: A global problem, *Kuwait med. J.* **2006**, *38*, 171-185, DOI: 10.4103/0974-777X.68531.

[41] Sun, L.; Zhang, L.; Zhang, H.; He, Z. G., Characterization of a bifunctional β-Lactamase/Ribonuclease and its interaction with a chaperon-like protein in the pathogen mycobacterium tuberculosis H37Rv, *Biochemistry.* **2011**, *76*, 350-358, DOI: 10.1134/S0006297911030096.

[42] Tamilselvi, A.; Mugesh, G.; Zinc and antibiotic resistance: metallo-β-lactamases and their synthetic analogues, *J. Biol. Inorg. Chem.* **2008**, *13*, 1039-1053, DOI: 10.1007/s00775-008-0407-2.

[43] Wang, Z.; Fast, W.; Benkovic, S. J., On the mechanism of the bacteroides fragilis metallo-β-

Lactamase, *Biochemistry*. **1999**, *38*, 10013-10023, DOI: 10.1021/bi990356r.

[44] Wang, Z.; Benkovic, S. J., Purification, characterization, and kinetic studies of a soluble bacteroides fragilis metallo-β-lactamase that provides multiple antibiotic resistance, *Biol. Chem.* **1998**, *273*, 22402-22408.

[45] Wang, Z.; Fast, W.; Benkovic, S. J., Direct observation of an enzyme-bound intermediate in the catalytic cycle of the metallo-β-lactamase from bacteroides fragilis, *J. Am. Chem. Soc.* **1998**, *120*, 10788-10789, DOI: 10.1021/ja982621m.

[46] Simm, A. M.; Loveridge, E. J.; Crosby, J.; Avison, M. B.; Walsh, T. R.; Bennett, P. M., Bulgecin A: a novel inhibitor of binuclear metallo-β-lactamases, *Biochem. J.* **2005**, *387*, 585-590, DOI: 10.1042/BJ20041542.

[47] Frisch, M. J.; Trucks, G. W.; Schlegel, H. B.; Scuseria, G. E.; Robb, M. A.; Cheeseman, J. R.; Zakrzewski, V. G.; Montgomery, J. A.; Stratmann, R. E.; Burant, J. C.; Dapprich, S.; Millam, J. M.; Daniels, A. D.; Kudin, K. N.; Strain, M. C.; Farkas, O.; Tomasi, J.; Barone, V.; Cossi, M.; Cammi, R.; Mennucci, B.; Pomelli, C.; Adamo, C.; Clifford, S.; Ochterski, J.; Petersson, G. A.; Ayala, P. Y.; Cui, Q.; Morokuma, K.; Malick, D. K.; Rabuck, A. D.; Raghavachari, K.; Foresman, J. B.; Cioslowski, J.; Ortiz, J. V.; Stefanov, B. B.; Liu, G.; Liashenko, A.; Piskorz, P.; Komaromi, I.; Gomperts, R.; Martin, R. L.; Fox, D. J.; Keith, T.; Al-Laham, M. A.; Peng, C. Y.; Nanayakkara, A.; Gonzalez, C.; Challacombe, M.; Gill, P. M. W.; Johnson, B. G.; Chen, W.; Wong, M. W.; Andres, J. L.; Head-Gordon, M.; Replogle, E. S.; Pople, J. A., Gaussian 98 (Revision A.1), Gaussian, Inc., Pittsburgh PA, 1998.

[48] Beck, A. D., Density-functional thermochemistry. III. The role of exact exchange, *J. Chem. Phys.* **1993**, *98*, 5648-5652, DOI: 10.1063/1.464913.

[49] Parr, R. G.; Yang, W., Density-functional theory of atoms and molecules. Oxford Univ. Press, Oxford, 1989.

[50] Tomasi, J.; Barone, V.; Cossi, M., Geometry optimization of molecular structures in solution by the polarizable continuum model, *J. Comp. Chem.* **1998**, *19*, 404-417, DOI: 10.1002/(SICI)1096-987X(199803)19:4<404::AID-JCC3>3.0.CO;2-W.

[51] Bebrone, C.; Metallo-β-lactamases [classification, activity, genetic organization, structure, zinc coordination] and their superfamily, *Biochem. Pharm.* **2007**, *74*, 1686-1701, DOI: 10.1016/ j.bcp.2007.05.021.

[52] McCall, K. A.; Huang, C.; Fierke, C. A., Function and mechanism of zinc metalloenzymes, *J. Nutr.* **2000**, *130*, 1437S-1446S.

[53] Kaminskaia, N. V.; Spingler, B.; Lippard, S. J.; Intermediate in β-Lactam Hydrolysis Catalyzed by a Dinuclear Zinc(II) Complex: Relevance to the Mechanism of Metallo-β-lactamase, *J. Am. Chem. Soc.* **2001**, *123*, 6555-6563.

[54] Fast, W.; Wang, Z.; Benkovic, S. J.; Familial mutations and zinc stoichiometry determine the rate-limiting step in nitrocefin hydrolysis by metallo- beta -lactamase from bacteroides fragilis, *Biochemistry.* **2001**, *40*, 1640-1650.

[55] Navarrete, M.; Rangel, C.; Corchado, J. C.; Espinosa-Garcia, J., Trapping of the OH radical by α-tocopherical: A theoretical study, *J. Phys. Chem.* A. **2005**, *109*, 4777-4784, DOI: 10.1021/jp050717e.

[56] Chandra, A. K.; Uchimaru, T., The O-H bond dissociation energies of substituted phenols and proton affinities of substituted phenoxide ions: a DFT study, *Int. J. Mol. Sci.* **2002**, *3*, 407-422, DOI: 10.3390/i3040407.

[57] [57] Zhang, H.Y.; Ji, H.F.; S-H proton dissociation enthalpies of thiophenolic cation radicals: a DFT study, *J. Mol. Struct: Theochem.* **2003**, *663*, 167-174, DOI: 10.1016/j.theochem.2003.08.124.